Regulation of the Actin Cytoskeleton Organization in Yeast by a Novel Serine/Threonine Kinase Prk1p

Guisheng Zeng and Mingjie Cai

Institute of Molecular and Cell Biology, National University of Singapore, Singapore 117609

Abstract. Normal actin cytoskeleton organization in budding yeast requires the function of the Pan1p/End3p complex. Mutations in *PAN1* and *END3* cause defects in the organization of actin cytoskeleton and endocytosis. By screening for mutations that can suppress the temperature sensitivity of a *pan1* mutant (*pan1-4*), a novel serine/threonine kinase Prk1p is now identified as a new factor regulating the actin cytoskeleton organization in yeast. The suppression of *pan1-4* by *prk1* requires the presence of mutant Pan1p. Although viable, the *prk1* mutant is unable to maintain an asymmetric distribution of the actin cytoskeleton at 37°C. Consistent with its role in the regulation of actin cytoskeleton, Prk1p localizes to the regions of cell growth and coincides with the polarized actin patches. Overexpression of the *PRK1* gene in wild-type cells leads to lethality and actin cytoskeleton abnormalities similar to those exhibited by the *pan1* and *end3* mutants. In vitro phosphorylation assays demonstrate that Prk1p is able to phosphorylate regions of Pan1p containing the LxxQxTG repeats, including the region responsible for binding to End3p. Based on these findings, we propose that the Prk1 protein kinase regulates the actin cytoskeleton organization by modulating the activities of some actin cytoskeleton-related proteins such as Pan1p/End3p.

Key words: actin cytoskeleton • cell polarity • EH domain • protein kinase • phosphorylation

THE actin cytoskeleton is involved in many fundamental cellular processes responsible for morphogenesis and development in eukaryotes. In the yeast *Saccharomyces cerevisiae*, the actin cytoskeleton is required for polarized cell growth, integrity of the cell wall, secretion and endocytosis, and a variety of other processes (for a recent review see Botstein et al., 1997). The role of the actin cytoskeleton as the determinant of growth polarity in yeast has been well established (Novick and Botstein, 1985; Harold, 1990; Kron and Gow, 1995; Drubin and Nelson, 1996; Botstein et al., 1997; Lew et al., 1997). The yeast actin cytoskeleton includes two types of structures visible by fluorescence light microscopy: the cortical actin patches and the cytoplasmic actin cables. These structures are highly dynamic, undergoing extensive rearrangements in accordance with polarity switches during the cell cycle. In unbudded G1 cells that grow isotropically, cortical actin patches are distributed randomly. Just before bud emergence, and coincident with the activation of the cyclin-dependent kinase Cdc28p at "Start," the actin patches are rapidly polarized to a small region on the cell cortex (Adams and Pringle, 1984; Kilmartin and Adams, 1984; Novick and Botstein, 1985; Lew and Reed, 1993, 1995; Welch et al., 1994; Kron and Gow, 1995). This step specifies the "pre-bud" site and its onset may require the activity of Cdc28p in complex with the Cln family of cyclins (Lew and Reed, 1993, 1995). After bud emergence, cortical actin patches remain inside the bud to maintain cell growth in a polarized fashion. The asymmetric distribution of the cortical actin continues until the time of mitosis, when cortical actin patches begin to redistribute randomly into both the mother and the bud. This is quickly followed by yet another rapid polarization of the actin cytoskeleton: the congregation of actin to the sides of the neck. This step is a prerequisite for cytokinesis and probably requires inactivation of the Cdc28p/Clb kinases (Lew and Reed, 1993, 1995).

The polarity switch before bud emergence also requires the function of the Rho family of GTPases including, notably, Cdc42p (Adams et al., 1990; Johnson and Pringle, 1990). Mutations in *CDC42* result in large, unbudded cells with a random distribution of cortical actin patches, a phenotype indicative of a defect in the polarity switch (Adams et al., 1990; Johnson and Pringle, 1990). Consistent with its role in the regulation of actin rearrangement, the Cdc42p

Address correspondence to Mingjie Cai, Institute of Molecular and Cell Biology, National University of Singapore, 30 Medical Drive, Singapore 117609. Tel.: (65)8743382. Fax: (65)7791117. E-mail: mcbcaimj@imcb.nus.edu.sg

protein is localized to the pre-bud site in unbudded cells and on the tip of the growing bud (Ziman et al., 1993).

The mechanisms underlying the rapid changes in cortical actin distribution have not been elucidated. On one hand, actin filaments in yeast have been shown to undergo rapid cycles of assembly and disassembly in vivo (Ayscough et al., 1997). On the other hand, visualization of fluorescently labeled actin cytoskeleton in living cells has led to the conclusion that cortical actin patches are highly mobile and can move across considerable distances on the cell cortex (Doyle and Botstein, 1996; Waddle et al., 1996). The ultrastructure of the actin patches has been investigated with the aid of immunoelectron microscopy and the patches are seen to comprise finger-like membrane invaginations surrounded by actin filaments (Mulholland et al., 1994). It is not yet clear how such a structure can be reconciled with the observed rapid motion of the actin patches in the plane of the plasma membrane.

Although the role for Cdc28p in the regulation of cell polarity during cell cycle progression is supported by some evidence (Benton et al., 1993; Cvrckova and Nasmyth, 1993; Lew and Reed, 1993, 1995; Tang and Cai, 1996), little is known about how this regulation is accomplished. By screening for mutants that lose viability rapidly in combination with the Start-defective *cdc28* mutation, we have identified a yeast protein, Pan1p, as required for normal organization of the actin cytoskeleton in yeast (Tang and Cai, 1996; Tang et al., 1997). At a restrictive temperature, the *pan1* mutant exhibited many phenotypes associated with defects in the actin cytoskeleton, such as abnormal bud growth, irregular structures of the actin cytoskeleton, and a random pattern of bud site selection (Tang and Cai, 1996). The Pan1p protein was found to colocalize with the cortical actin patches (Tang and Cai, 1996; Tang et al., 1997). Structurally, Pan1p contains a domain homologous to another yeast protein, Sla1p, that is also required for normal actin cytoskeleton organization (Holtzman et al., 1993, 1994; Li et al., 1995; Tang and Cai, 1996). Pan1p also has two repeats of a newly identified protein motif known as the EH domain, for its homology with the mammalian protein Eps15 which has been implicated in the process of receptor-mediated endocytosis (Tang and Cai, 1996; Di Fiore et al., 1997). Another yeast EH domain–containing protein, End3p (Bénédetti et al., 1994; Tang and Cai, 1996), was later found to form a complex with Pan1p in vivo (Tang et al., 1997). Genetic and molecular studies have shown that the Pan1p/End3p complex is essential for both the organization of actin cytoskeleton and endocytosis (Tang and Cai, 1996; Tang et al., 1997).

In this study, we have searched for additional factors that may interact with, or regulate the activity of, the Pan1p/End3p complex, by screening for extragenic suppressors of *pan1*. One such suppressor is found to be *prk1*. The wild-type *PRK1* gene encodes a novel serine/threonine kinase. Our data suggest that Prk1p is an important regulator of the actin cytoskeleton organization in yeast, and that one of its functions in the regulation of the actin cytoskeleton is to negatively control the activity of the Pan1p/End3p complex.

Materials and Methods

Strains, Media, and General Methods

The yeast strains used in this study are listed in Table I. All strains are derived from W303. YMC425, YMC426, and YMC427 were made by disrupting the *PRK1* gene in YMC422, YMC423, and W303-1A, respectively. YMC428 was a progeny of a diploid made of a cross between YHT151 and YMC427. YMC429 and YMC430 were made by crossing YMC424 with YMC423 and YMC426, respectively. Rich (YPD), synthetic complete (SC), and dropout media were prepared as described (Rose et al., 1990). Temperature-sensitive mutants were propagated at the permissive temperature of 23°C and analyzed at the restrictive temperature of 37°C. Genetic manipulations were performed according to standard methods described by Rose et al. (1990). Recombinant DNA methodology was performed as described by Sambrook et al. (1989).

Isolation of pan1-4 Spontaneous Revertants

Spontaneous revertants of *pan1-4* were selected by plating 1.58×10^8 of *pan1-4* (YMC422, Table I) cells on YPD plates and keeping the plates at 37°C for 2 d. Colonies that could grow under these conditions were picked up, colony-purified, and tested for their growth at 37°C once again. Good candidates were crossed with the wild-type strain W303. The diploid cells so formed were sporulated and tetrad-dissected and their progeny cells were tested for temperature sensitivity at 37°C to distinguish the extragenic mutations from the intragenic ones. The extragenic revertants were then crossed with a *pan1-4* mutant (YMC423, Table I) to test whether the suppressor mutation was recessive. Revertant 1 (YMC424, Table I), which carried an extragenic recessive mutation and showed good viability at 37°C, was the subject of this study.

Cloning of the PRK1 Gene

The strain YMC424 was transformed with a yeast genomic library constructed in the plasmid pRS315 (Sikorski and Hieter, 1989). Approxi-

Table I. Yeast Strains

Strain	Genotype	Reference
W303-1A	*MAT* **a** *ade2-1 trp1-1 can1-100 leu2-3,112 his3-11,15 ura3-1*	This study
W303-1B	*MAT* α *ade2-1 trp1-1 can1-100 leu2-3,112 his3-11,15 ura3-1*	This study
YHT151	*MAT* α *ade2 trp1 can1 leu2 his3 ura3 end3Δ::LEU2*	Tang et al., 1997
YMC422	*MAT* **a** *ade2 his3 leu2 trp1 ura3 pan1-4*	This study
YMC423	*MAT* α *ade2 his3 leu2 trp1 ura3 pan1-4*	This study
YMC424	*MAT* **a** *ade2 his3 leu2 trp1 ura3 pan1-4 prk1-1*	This study
YMC425	*MAT* **a** *ade2 trp1 can1 leu2 his3 ura3 pan1-4 prk1Δ::URA3*	This study
YMC426	*MAT* α *ade2 trp1 can1 leu2 his3 ura3 pan1-4 prk1Δ::URA3*	This study
YMC427	*MAT* **a** *ade2 trp1 can1 leu2 his3 ura3 prk1Δ::URA3*	This study
YMC428	*MAT* **a** *ade2 trp1 can1 leu2 his3 ura3 end3Δ::LEU2 prk1Δ::URA3*	This study
YMC429	*MAT* **a**/α *pan1-4/pan1-4 prk1-1/PRK1*	This study
YMC430	*MAT* **a**/α *pan1-4/pan1-4 prk1-1/prk1Δ::URA3*	This study

mately 20,000 transformants were obtained. They were then tested for temperature sensitivity at 37°C. Plasmids from the temperature-sensitive transformants were extracted and were reintroduced into YMC424 to confirm the ability to confer temperature sensitivity. One of the plasmids that passed these tests was sequenced and revealed to contain the *PRK1* gene. Further analysis confirmed that *PRK1* was required for the complementation of the suppressor mutation in YMC424.

Plasmid Constructs

pPRK1 was generated by inserting a 3.9-kb fragment containing the *PRK1* gene (base pair number −1190 to 2740) into the SacI/KpnI site of pRS314. pGAL-PRK1 was made by adding a SacI site in front of the initiation codon and an XbaI site in the 3′-end region of the *PRK1* gene by PCR. The 2.7-kb SacI/XbaI fragment, covering the full length of *PRK1*, was cloned into the SacI/XbaI sites just downstream of the *GAL1* promoter in three vectors derived from pRS314, pRS315, and pRS316, respectively. To construct pGAL-HA-PRK1, a unique AscI site was generated by PCR immediately after the initiation codon of *PRK1*. A 2.7-kb *PRK1* fragment was excised with AscI/SalI digestion and its 5′-end was fused in frame with a sequence encoding three tandem repeats of the HA epitope (YPYDVPDYAG) downstream of the *GAL1* promoter in two vectors derived from pRS314 and pRS316, respectively. pHA-PRK1, a construct containing the HA-tagged *PRK1* driven by the endogenous promoter, was generated by replacing the *GAL1* sequence in pGAL-HA-PRK1 with the *PRK1* promoter (base pair number −976 to −1). The pRS314-related pGAL-HA vector was also used to tag the second long repeat (residues 384–846) of Pan1p (pGAL-HA-LR2), which served as an in vivo substrate for Prk1p as described in Fig. 5 D.

Disruption of the PRK1 Gene

The *PRK1* gene was disrupted by the one-step gene replacement method (Rothstein, 1991). The *PRK1* coding region between the BclI site and the SpeI site was removed and replaced by the *URA3* marker. The *URA3* gene flanked by *PRK1* sequences (*prk1Δ::URA3*) was excised by SalI and HindIII digestion, followed by gel purification and transformation into the wild-type strain W303, as well as the *pan1-4* mutant (YMC422 and YMC423). The deletion was confirmed by PCR analysis.

Cell Morphology and FACScan® Studies

The yeast cultures were synchronized by addition of α-factor to a final concentration of 8 μg/ml. After incubation at 23°C for 2 h, most cells were arrested in G1 as unbudded cells. The measurement of cell morphology and DNA content by FACScan® analysis was carried out as described previously (Li and Cai, 1997).

Fluorescence Studies

Staining of actin filaments using rhodamine-phalloidine and determination of protein subcellular localization by antibody staining followed the published procedure (Tang and Cai, 1996). To visualize the HA-tagged Prk1p, the mouse mAb 12CA5 (Boehringer Mannheim) was used as the primary antibody, and the rhodamine-conjugated goat anti–mouse IgG (Jackson ImmunoResearch) as the secondary antibody. To costain HA-Prk1 and actin, the antibodies were used in the following order: mouse anti-HA, guinea pig antiactin, rhodamine-conjugated goat anti–mouse IgG, and finally fluorescein-conjugated donkey anti–guinea pig IgG. In control experiments, no cross-reactivity was observed between the following pairs of antibodies: the mouse anti-HA antibody and the fluorescein-conjugated donkey anti–guinea pig IgG, the guinea pig antiactin antibody and the rhodamine-conjugated goat anti–mouse IgG, and the rhodamine-conjugated goat anti–mouse IgG and fluorescein-conjugated donkey anti–guinea pig IgG.

Immunoprecipitation, GST-Fusion Proteins, Oligopeptides, and In Vitro Kinase Assay

The immunoprecipitation of proteins from yeast extracts followed the procedure published in detail previously (Tang et al., 1997). To treat the immunoprecipitates with calf intestinal alkaline phosphatase (CIP),[1] the protein A–Sepharose beads were washed with RIPA buffer (50 mM Tris-HCl, pH 7.2, 1% Triton X-100, 1% sodium deoxycholate, 0.1% SDS, 150 mM NaCl), followed by incubation at 37°C with 1 μl of 10 U/μl CIP (Biolabs, Inc.) for 30 min and boiling in the sample buffer.

To make glutathione *S*-transferase (GST)-fusion proteins, various coding regions of *PAN1* (LR1: residues 99–383; LR2: 383–900; poly-P: 1239–1480; R15T and R15G: 564–846; R15Δ: 576–846) and *END3* (full length) were generated by PCR and fused in-frame to a bacterial GST expression vector pGEX-4T-1 (Pharmacia). The plasmids were transformed into *Escherichia coli* BL21. Transformants were grown to OD_{600} = 0.5, and induced with 1 mM isopropylthio-β-d-galactoside (Life Technologies, Inc.) at 37°C for 4 h to express the fusion proteins. Cells were collected by centrifugation and suspended in cold PBS. The suspensions were sonicated on ice to lyse the cells and the lysates were centrifuged at 10,000 rpm for 10 min in a Sorvall SS-34 rotor. The supernatants were incubated with glutathione–Sepharose 4B beads (Pharmacia) for 30 min at room temperature, then transferred to disposable columns (Pharmacia). The beads were washed with PBS three times and the fusion proteins were eluted from the beads by elution buffer (10 mM glutathione, 50 mM Tris-HCl, pH 8.0).

For protein kinase assays, the polyclonal rabbit anti-HA antibody was used to precipitate HA-tagged Prk1p. The beads were first washed with the RIPA buffer for five times, then three times with 25 mM MOPS (pH 7.2) and resuspended in 6 μl of HBII buffer (60 mM β-glycerophosphate, 25 mM MOPS, pH 7.2, 15 mM *p*-nitrophenylphosphate, 15 mM $MgCl_2$, 5 mM EGTA, 1 mM dithiothreitol, 1 mM phenylmethylsulfonyl fluoride, 20 μg leupeptin/ml, and 0.1 mM sodium orthovanadate). The kinase assay was performed by incubating the beads with 5 μg of GST-fusion proteins, 0.5 μl of 1 mM ATP, 0.5 μl of [γ-^{32}P]ATP (10 mCi/ml; New England Nuclear Inc.), 1 μl of 250 mM MOPS in a total volume of 20 μl at 25°C for 15 min, followed by addition of 3× loading buffer and 10% SDS-PAGE. The gels were first stained with Coomassie blue to visualize the protein bands. After pictures were taken, the gels were fixed, dried, and exposed to x-ray films.

Oligopeptides (RP15: MPLTAQKTGFGNNE; Q6A: MPLTAAKTGFGNNE; T8A: MPLTAQKAGFGNNE; and G9A: MPLTAQKTAFGNNE) were synthesized by a commercial company (Research Genetics) and dissolved in 2.5 mM MOPS to a concentration of 5 μg/μl. Silver staining was used to visualize the peptides in SDS-polyacrylamide gels. Equal amounts of each peptide (60 μg) were used for the kinase assay. After electrophoresis on a 16.5% SDS-polyacrylamide gel, the peptides were transferred to a polyvinylidene fluoride (PVDF) membrane (Millipore, Inc.) and followed by autoradiography.

Site-directed Mutagenesis of Prk1p

The in vitro site-directed mutagenesis was performed using the Transformer™ site-directed mutagenesis kit from Clontech. The plasmid pPRK1-314 was used as the template for generating pPRK1^{D158Y}. The mutagenic primer used to create a D to Y mutation in *PRK1* was CGCCATTGATTCATcGAtATATTAAGATTGAG, which also created a ClaI site because of the mutation. The selection primer for the SnaBI site of the pRS314 vector was GCTTGTCACCTgACGTcCAATCTTGATCC. The mutation was first detected by restriction digestion and then confirmed by DNA sequencing. To create pGAL-PRK1^{D158Y} and pGAL-HA-PRK1^{D158Y}, the SacI/PstI fragment of pPRK1^{D158Y} containing the promoter region and some NH_2-terminal sequences of *PRK1* was replaced by the SacI/PstI fragments from pGAL-PRK1 and pGAL-HA-PRK1, respectively.

Results

prk1 Is an Extragenic Suppressor of pan1-4

The *pan1-4* mutation causes a temperature-dependent growth defect (Tang and Cai, 1996). To isolate spontaneous revertants of *pan1-4*, the mutant cells (YMC422, Table I) were plated on YEPD plates and incubated at 37°C for several days. Eight revertants were found to grow on these plates. After colony purification, these cells were retested for the ability to grow at 37°C. These spontaneous revertants could, in principle, arise from either additional muta-

1. *Abbreviations used in this paper:* CIP, calf intestinal alkaline phosphatase; GST, glutathione *S*-transferase.

tions in *pan1-4*, or mutations in other genes. To distinguish the intragenic suppressors from the extragenic ones, each of the eight revertants was crossed with a wild-type strain (W303-1B, Table I), and the diploids were subjected to sporulation and tetrad dissection. The progeny cells were tested for temperature sensitivity. The result showed that all of the revertant strains carried extragenic mutations (data not shown). Revertant 1 (YMC424, Table I) was chosen for further studies because it grew better at 37°C than the others. Fig. 1 A shows the suppression of the temperature sensitivity of *pan1-4* in YMC424. Cloning of the suppressor gene was achieved by transforming YMC424 with a yeast genomic library and screening for transformants that exhibited plasmid-dependent temperature sensitivity at 37°C. The plasmid in these temperature-sensitive cells was extracted and used again for transformation of YMC424 to confirm its ability to complement the suppressor mutation. Upon sequence analysis, the suppressor gene was identified as *PRK1*.

PRK1 (YIL095W) is registered in the Yeast Protein Database (www.proteome.com) as a nonessential gene encoding a putative serine/threonine kinase with unknown functions. Since it is important to know whether loss of Prk1p function will result in suppression of the *pan1-4* mutation, a null mutation of *prk1* was generated. The *PRK1* gene in a wild-type (W303) as well as in a *pan1-4* strain (YMC422) was disrupted by the one-step gene replacement method using *URA3* as a marker (Rothstein, 1991). As shown in Fig. 1 B, *prk1Δ* was able to suppress the temperature sensitivity of *pan1-4*, as the *prk1Δ pan1-4* double mutant (YMC425, Table I) could grow at 37°C. In agreement with the earlier report (Thiagalingam et al., 1995), the *prk1Δ* mutant (YMC427, Table I) was viable.

To ensure that *PRK1* was allelic to, rather than just a suppressor of, the mutation in revertant 1 that caused the suppression of *pan1-4*, we crossed revertant 1 with the *prk1Δ pan1-4* double mutant. As shown in Fig. 1 C, the diploid thus formed was viable at 37°C. In contrast, the diploid generated by crossing revertant 1 with *pan1-4* was still temperature sensitive at 37°C (Fig. 1 C). This result shows that the mutation responsible for the suppression of *pan1-4* in revertant 1 is recessive, and is indeed allelic to *PRK1*. Therefore, we named the mutation in revertant 1 that caused the *pan1-4* suppression as *prk1-1*.

However, *prk1* could not suppress the lethality of the null mutation of *pan1*. This result was obtained by crossing the *prk1Δ* mutant with the *pan1Δ* mutant, whose viability was maintained by the wild-type *PAN1* gene on a plasmid. After sporulation and tetrad dissection, it was found that all the viable spore colonies that carried both markers for *prk1* and *pan1* disruption (*URA3* and *HIS3*) always carried the marker for the *PAN1*-containing plasmid, *LEU2* (data not shown). Furthermore, these Ura^+ His^+ Leu^+ cells were incapable of losing the *PAN1*-containing plasmid despite continuous propagation in the liquid rich medium (YPD) for several days (data not shown). These results indicate that the presence of the *prk1Δ* mutation offers no relief to the absolute dependence of the *pan1Δ* cells on the *PAN1* gene, and suggest that *prk1Δ* does not result in a bypass of the Pan1p function in the cell.

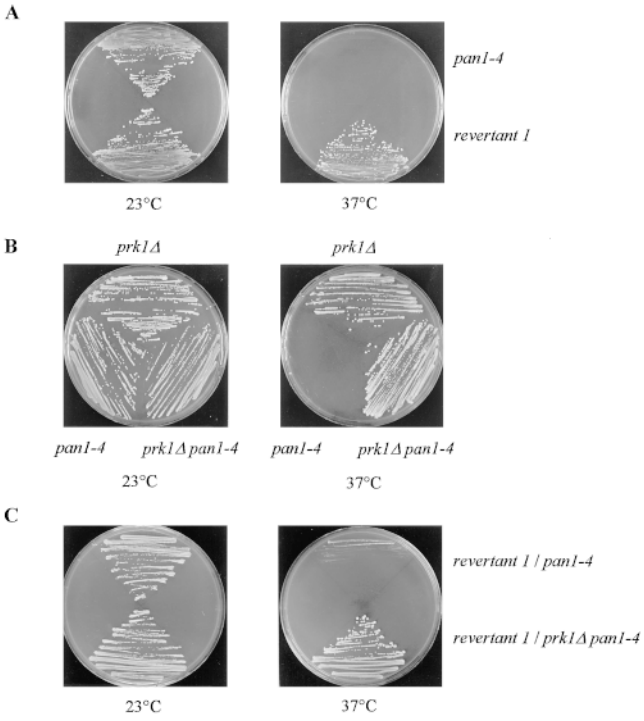

Figure 1. Suppression of the temperature sensitivity in *pan1-4* by the *prk1-1* and *prk1Δ* mutations. (A) The strains of YMC422 (*pan1-4*) and revertant 1 (YMC424, *prk1-1 pan1-4*) were tested for growth at 23°C (left) and 37°C (right). (B) The strains of YMC427 (*prk1Δ*), YMC422 (*pan1-4*), and YMC425 (*prk1Δ pan1-4*) were tested for growth at 23°C (left) and 37°C (right). (C) The diploid strains of YMC429 (*pan1-4 prk1-1*/*pan1-4 PRK1)* and YMC430 (*pan1-4 prk1-1*/*pan1-4 prk1Δ*) were tested for growth at 23°C (left) and 37°C (right). All strains were streaked on YPD plates and incubated at respective temperatures for 3 d.

Actin Abnormalities in pan1-4 and prk1Δ Are Corrected in the Double Mutant

Given the allele-specific suppression of *pan1-4* by *prk1*, it is anticipated that Prk1p may be required for certain functions of the actin cytoskeleton, even though it is nonessential for viability. This possibility was investigated first by examining the *prk1Δ* mutant (YMC427) for any visible disorganization of the actin cytoskeleton. Although a normal pattern of cortical actin distribution was seen in the mutant cells grown at 23°C (Fig. 2 A, left), it was evident that most (>80%) of *prk1Δ* mutant cells grown at 37°C had lost the asymmetric localization of the cortical actin patches characteristic of wild-type cells (Fig. 2 A, right). Actin patches in *prk1Δ* cells were more or less evenly distributed between the mother and the bud. The depolarization of the actin patches in *prk1Δ* cells was not a result of the treatment at 37°C per se, as the wild-type cells basically retained their polarized actin distribution after the same treatment (data not shown). In addition to the depolarized distribution of the cortical actin patches, the cycling *prk1Δ* cell population accumulated more unbudded cells at 37°C than the wild-type cells. As cortical actin polarization is required for budding (Novick and Botstein,

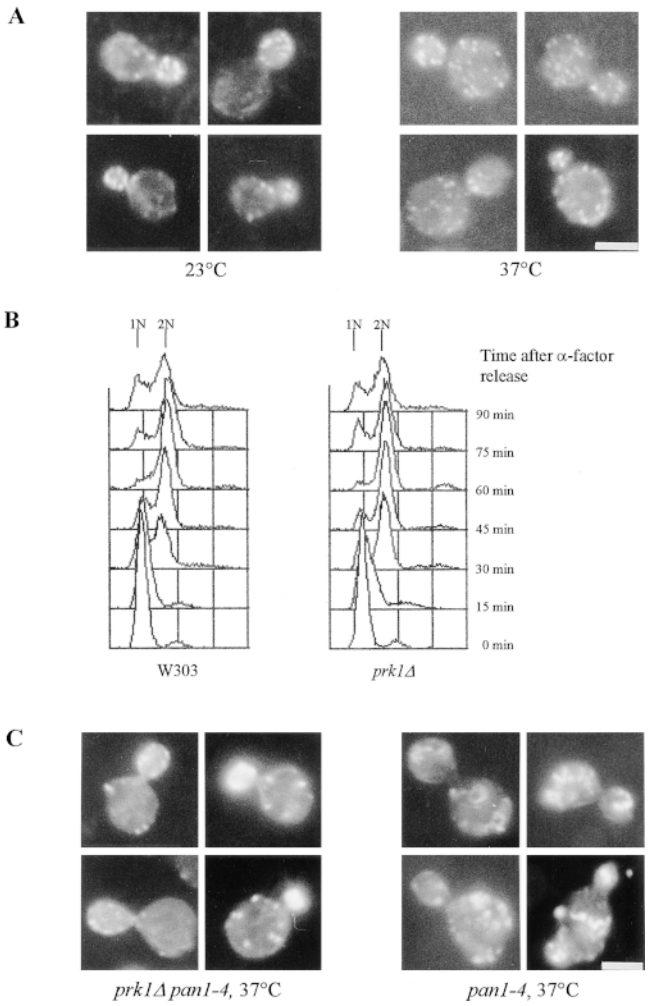

Figure 2. Phenotypes of *prk1Δ* and *prk1Δ pan1-4* mutants. (A) Rhodamine-phalloidin staining of actin filaments in the *prk1Δ* mutant (YMC427) growing at 23°C (left), and at 37°C for 5 h (right). (B) Flow cytometry analysis of the *prk1Δ* mutant at 37°C after release from α-factor arrest. Wild-type (W303) and *prk1Δ* (YMC427) cells were treated with α-factor for 2 h, followed by washing and resuspending the cells in fresh media prewarmed to 37°C. Samples were taken at a 15-min interval. (C) Rhodamine-phalloidin staining of actin filaments in the *prk1Δ pan1-4* mutant (YMC425, left) and the *pan1-4* mutant (YMC422, right) after 5 h of incubation at 37°C. Bar, 4 μm.

1985; Drubin and Nelson, 1996; Botstein et al., 1997), we reasoned that a defect in polarization of the actin patches might have affected bud formation in the mutant. To determine whether this was the case, we examined the timing of budding relative to the timing of DNA synthesis in *prk1Δ* and wild-type cells using α-factor–synchronized cultures. As shown in Fig. 2 B, *prk1Δ* cells initiated DNA synthesis at about the same time as the wild-type control after release from α-factor arrest. However, bud emergence and bud growth in the mutant were significantly delayed (Table II). 15 min after release, for example, 26% of the wild-type cells had formed buds whereas only 13% of mutant cells had done so (Table II). Even 30 min later, the mutant population still contained 36% unbudded cells, compared

Table II. The Budding Profiles of the prk1Δ Mutant after Release to 37°C from α-factor Arrest

Time	Strain	% of cells (mean ± SD) with: No bud	Small bud	Large bud
min				
0	Wild type	98.5 ± 0.5	0	1.5 ± 0.5
	prk1Δ	98.5 ± 0.5	0	1.5 ± 0.5
15	Wild type	74.0 ± 3.0	26.0 ± 3.0	0
	prk1Δ	87.0 ± 3.0	13.0 ± 3.0	0
30	Wild type	37.5 ± 0.5	61.5 ± 1.5	1.0 ± 1.0
	prk1Δ	49.5 ± 1.5	49.5 ± 0.5	1.0 ± 1.0
45	Wild type	21.0 ± 4.0	76.5 ± 5.5	2.5 ± 1.5
	prk1Δ	36.3 ± 3.0	62.5 ± 4.5	1.5 ± 1.5
60	Wild type	9.0 ± 1.0	34.5 ± 3.5	56.5 ± 4.5
	prk1Δ	10.0 ± 1.0	51.5 ± 1.5	38.5 ± 0.5
75	Wild type	7.0 ± 1.0	24.5 ± 0.5	68.5 ± 0.5
	prk1Δ	10.0 ± 1.0	37.0 ± 3.0	53.0 ± 2.0
90	Wild type	25.0 ± 1.0	24.5 ± 3.5	51.0 ± 5.0
	prk1Δ	27.5 ± 1.5	33.5 ± 2.5	39.0 ± 4.0

with 21% unbudded cells in the wild-type population (Table II). In view of the normal timing of initiation of DNA replication in the mutant, the accumulation of unbudded cells in the *prk1Δ* population cannot be accounted for by a defect in passage through Start. Rather, it must result from a defect specific for bud formation, possibly the mutant's inability to efficiently polarize actin patches.

The finding that *prk1* suppressed the *pan1-4* mutation but not the *pan1* null mutation suggests that the essential function of Pan1p had been restored in the mutant due to the loss of Prk1p function. To test whether the actin cytoskeleton defects in the *pan1-4* mutant were corrected by *prk1*, we examined the pattern of actin staining in the double mutant. As shown in Fig. 2 C, combination of the *pan1-4* and *prk1Δ* mutations brought the cortical actin distribution back to normality in most, if not all, of the double mutant cells. These cells (YMC425) exhibited an asymmetric distribution of the actin cytoskeleton at 37°C, with the majority of the actin staining being concentrated in the bud (Fig. 2 C, left). The prominent abnormal actin staining inside the mother cell in the *pan1-4* mutant (Fig. 2 C, right) was no longer present in the double mutant. These results indicate that the suppression of *pan1-4* by *prk1* is due, at least in part, to a normalization of the actin cytoskeleton organization in the *pan1-4* mutant by the loss of Prk1p function.

PRK1 Overexpression Is Lethal

Although cells could survive with the *PRK1* gene deleted, overproduction of Prk1p was lethal. As shown in Fig. 3 A, W303 cells that contained the *PRK1* gene under the control of the *GAL1* promoter (pGAL1-PRK1) could not grow on plates with galactose as the carbon source. The lethality of *PRK1* overexpression was likely a result of defective actin cytoskeleton, since the actin cytoskeleton was grossly altered in these cells (Fig. 3 B). After several hours in galactose, most of these cells accumulated aberrant actin aggregates, such as thick, and sometimes curvy, bars and larger than normal patches, with very few normal looking actin patches on the cortex (Fig. 3 B, right). These

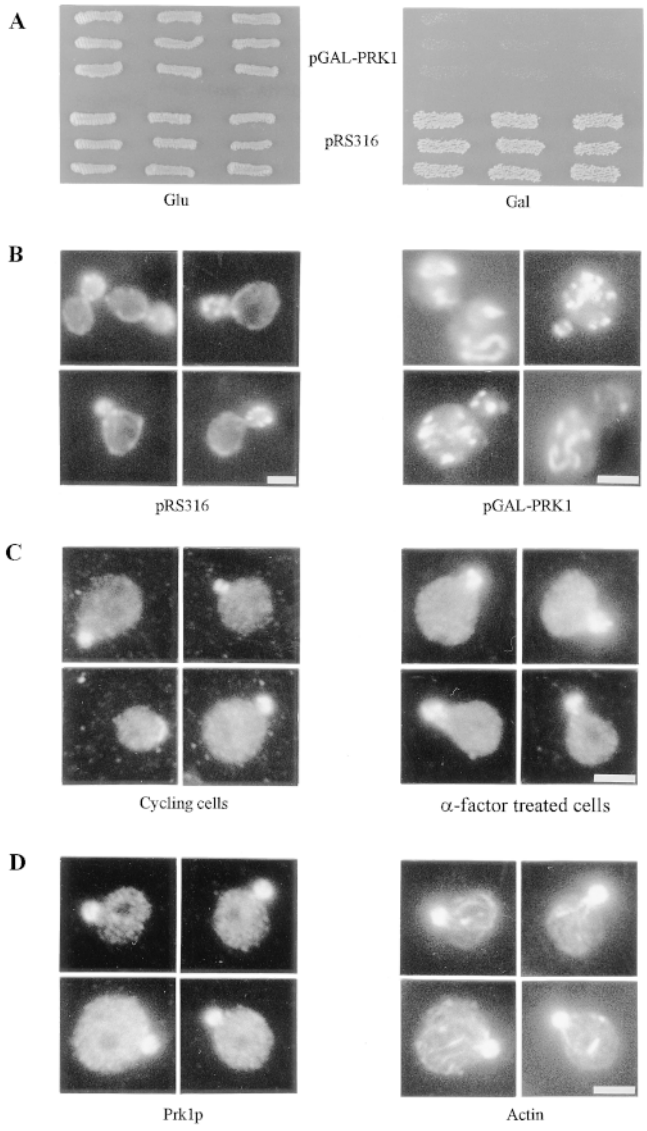

Figure 3. Prk1p overproduction and subcellular localization. (A) W303 cells containing pGAL-PRK1 and the control vector pRS316, respectively, were grown first on a glucose-containing Ura-dropout plate (left) and then replica-plated on a galactose-containing Ura-dropout plate (right). Photographs were taken after each plate was incubated at 30°C for 2 d. (B) Rhodamine-phalloidin staining of actin filaments in W303 cells containing a control vector pRS316 (left) and pGAL-PRK1 (right). Cells were processed for fluorescent staining after 5 h of incubation in galactose-containing medium. (C) Subcellular localization of Prk1p in cycling cells (left) and α-factor–arrested cells (right). W303 cells containing pGAL-HA-PRK1 were exposed to galactose or galactose plus α-factor for 90 min before being processed for immunofluorescent staining. Note that Prk1p localized to the pre-bud site in the unbudded cell. (D) Polarized localization of Prk1p and the actin filaments. (Left) Localization of Prk1p by the indirect immunofluorescence with anti-HA antibody. (Right) Localization of actin filaments with antiactin antibody. Bar, 4 μm.

aberrant actin structures are, to a large extent, reminiscent of those exhibited by the *pan1-4* and *end3Δ* mutants incubated at the restrictive temperature (Fig. 2 C, right) (Bénédetti et al., 1994; Tang and Cai, 1996; Wendland et al., 1996). Therefore, it appears that loss of Pan1p/End3p functions and overexpression of *PRK1* exert similar effects on the organization of actin cytoskeleton.

Cells overexpressing *PRK1* were found dead at all stages of the cell cycle (data not shown), and thus the lethality is unlikely attributable to any cell cycle–specific defects.

Prk1p Localizes to the Region of Polarized Growth

To obtain further insights into the function of Prk1p, we next attempted to determine the subcellular localization of Prk1p. To facilitate the detection of Prk1p in vivo, the *PRK1* gene expressed from its endogenous promoter was tagged with the HA epitope at the 5′-end. The HA-PRK1 construct thus formed was functional in vivo as it could restore the temperature sensitivity of the *prk1-1 pan1-4* (YMC424) or *prk1Δ pan1-4* (YMC425) double mutants (data not shown). However, this HA-PRK1 construct produced signals too weak to permit unambiguous detection by indirect immunofluorescent staining (data not shown). Thus, we opted to use the *GAL1* promoter. Cells containing the HA-tagged *PRK1* gene under *pGAL1* were not viable in galactose and exhibited the aberrant actin structures similar to those seen in the cells overexpressing untagged *PRK1* (data not shown). A transient exposure to galactose (90 min) was found to be sufficient to allow detection of the Prk1 protein by immunofluorescent staining using anti-HA antibody without causing significant actin abnormalities in cells containing this construct. In cycling cells, Prk1p appeared mostly at the regions of cell growth, such as small buds and tips of the oval-shaped unbudded cells indicative of the pre-bud sites (Fig. 3 C, left). Similarly, the Prk1p-specific staining was confined to the tip region of the shmoos in α-factor–arrested cells (Fig. 3 C, right). The Prk1p-specific staining was also found to coincide with polarized cortical actin patches, as shown in Fig. 3 D.

However, we were unable to ascertain whether Prk1p colocalized generally with the cortical actin patches, as Prk1p was mostly detected in cells with a polarized pattern of Prk1p localization. In cells that displayed randomly distributed actin patches, the staining of HA-Prk1p was significantly weaker (data not shown). It is not yet clear whether this is due to the experimental protocol or the nature of Prk1p subcellular localization.

Prk1p Phosphorylates the LxxQxTG Repeats in Pan1p

Prk1p belongs to a family of putative serine/threonine kinases. Fig. 4 A shows the sequence alignment of the kinase domain from five such kinases, with three from *S. cerevisiae*, one from *S. pombe*, and one from *Arabidopsis*. So far, these putative kinases have not been subjected to functional studies. *PRK1* was isolated previously in an artificial system as a gene that, when present in a high copy plasmid, could suppress the transcriptional defects of human p53-activated transcriptional units in six unidentified yeast mutants (Thiagalingam et al., 1995). How this suppression took place, however, was not investigated. Indeed, Prk1p has never been demonstrated to possess a protein kinase activity. Our finding that the suppression of *pan1-4* by *prk1* was dependent on the presence of the mutant Pan1

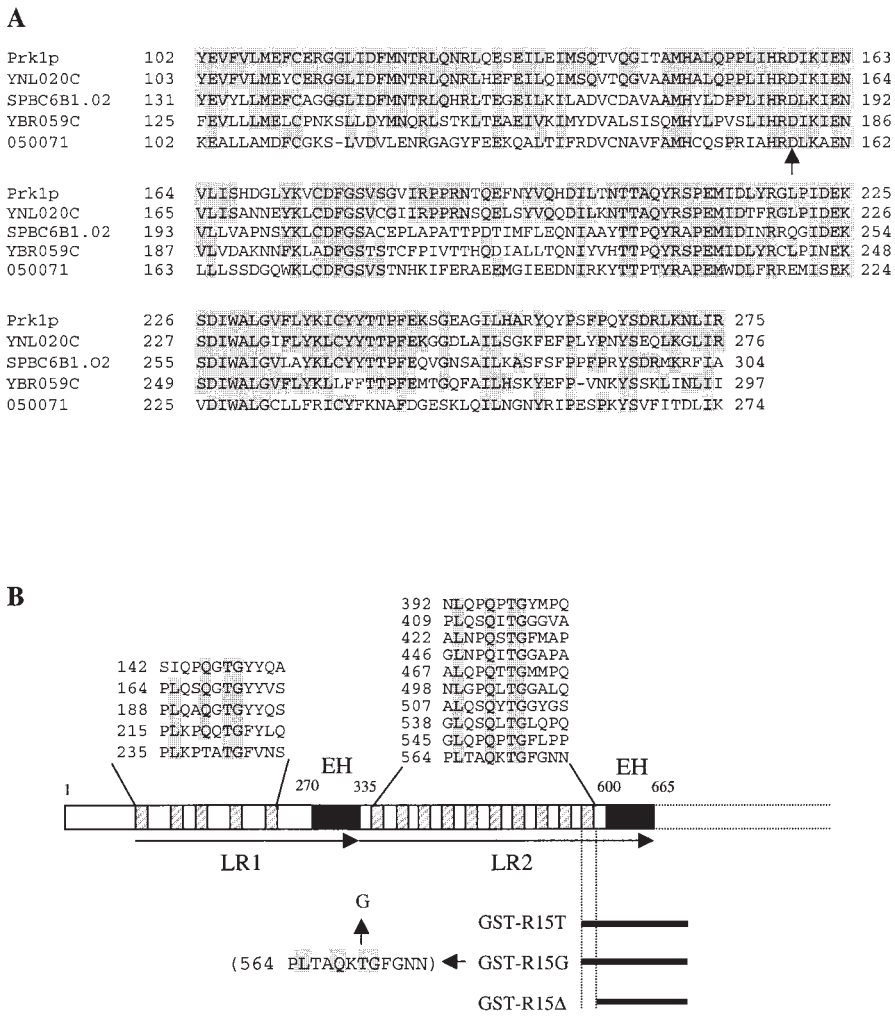

Figure 4. Alignment of the kinase domain from the Prk1 family of putative kinases and the analysis of the Pan1p structure in the LR1/LR2 region. (A) Alignment of the kinase regions from Prk1p and two other putative kinases from *S. cerevisiae*, YNL020C and YBR059C, one putative kinase from *S. pombe*, SPBC6B1.02 (AC, TrEMBL O43066), and one from *Arabidopsis* (AC, TrEMBL O50071). Residues conserved between Prk1p and others are highlighted. The arrow indicates the catalytic site D158 in Prk1p. (B) The analysis of the long repeats in Pan1p. The black bars below the diagram represent the regions of Pan1p used for making GST-fusion proteins. The Pan1 repeats (LxxQxTG) are marked as hatched boxes and the EH domains as solid boxes. The positions of each Pan1 repeat are shown above the diagram.

protein suggested that Prk1p may regulate Pan1p by phosphorylation. We tested this idea by setting up an in vitro kinase assay using various regions of Pan1p as substrates. The Pan1p protein can be divided into three parts according to its structural features: the NH_2-terminal long repeat one (LR1), the adjacent long repeat two (LR2), and the COOH-terminal proline-rich region (poly-P) (Tang and Cai, 1996). Three GST-fusion proteins were made from the above Pan1p regions and used in the in vitro kinase assay. As shown in Fig. 5 A, the immunoprecipitated Prk1p could indeed act as a protein kinase, phosphorylating both LR1 and LR2 efficiently. However, Prk1p could not phosphorylate the proline-rich region (Fig. 5 A, lane c). No LR2 phosphorylation was observed in the reaction where immunoprecipitates from cells containing untagged Prk1p were used (Fig. 5 A, lane f), indicating that the kinase reaction is specific to Prk1p. Since both LR1 and LR2 contain an EH domain in which there is a single conserved serine residue (Tang and Cai, 1996), it was initially thought that the EH domain might be the region recognized by the kinase. This turned out not to be the case, as another EH domain–containing protein, End3p, could not be phosphorylated by Prk1p (Fig. 5 A, lane d). Aside from the EH domain, another striking structural feature common to both LR1 and LR2 is the LxxQxTG motif, repeated 5 times in LR1 and 10 times in LR2 (Fig. 4 B). As this motif (named the Pan1 repeat) contains a conserved threonine, we investigated whether this is the phosphorylation site for Prk1p. Three additional GST-fusion proteins were made for this purpose. GST-R15T contained the LR2 fragment with all but one (the 15th) of the Pan1 repeats deleted. GST-R15G contained the same LR2 fragment as GST-R15T, but with the threonine in the remaining Pan1 repeat mutated to glycine (Fig. 4 B). GST-R15Δ differed from the above two in containing no Pan1 repeat (Fig. 4 B). The results of kinase assays using these three fusion proteins are shown in Fig. 5 B. Of the three fragments, only GST-R15T could be phosphorylated by Prk1p (Fig. 5 B). This demonstrates that the threonine residue in the LxxQxTG motif was critical in defining the phosphorylation target site of Prk1p.

It could be argued, perhaps, that the Pan1 repeat may just serve as a recognition site, rather than a phosphorylation site, for Prk1p. To prove that the LxxQxTG motif was the actual site phosphorylated by Prk1p, four oligopeptide substrates were synthesized for the kinase assay. These peptides, of 14 amino acids in length, were from the 15th Pan1 repeat as present in GST-R15T described above. As

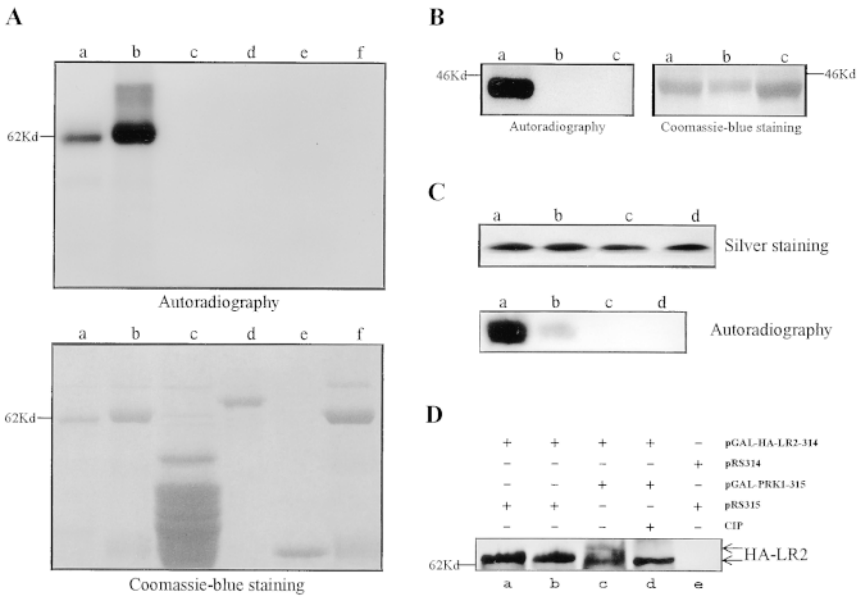

Figure 5. Phosphorylation of Pan1p by Prk1p. (A) In vitro phosphorylation of Pan1p by Prk1p. Phosphorylation results were shown in the upper panel as autoradiography and the input substrates were visualized by the Coomassie blue staining of the same gel shown in the lower panel. Immunoprecipitated HA-tagged Prk1p was added in lanes a–e as the kinase. In lane f, immunoprecipitates from cells containing untagged Prk1p were used as a control. Substrates used in lanes a–f were GST-LR1, GST-LR2, GST-polyP, GST-End3, GST, and GST-LR2, respectively. (B) Identification of the Prk1p phosphorylation site in Pan1p. Immunoprecipitated HA-tagged Prk1p was added in lanes a–c as the kinase. The phosphorylation results were shown in the left as autoradiography. The input substrates GST-R15T, GST-R15G, and GST-R15Δ in lanes a–c, respectively, were visualized by the Coomassie blue staining of the same gel shown in the right. (C) Confirmation of the Prk1p phosphorylation site by using oligopeptide substrates. Peptides RP15, Q6A, T8A, and G9A in lanes a–d were visualized by silver staining shown in the upper panel. The phosphorylation results were shown in the lower panel as autoradiography. Immunoprecipitated HA-tagged Prk1p was added in each lane as the kinase. Each reaction used the same quantity of oligopeptides (60 μg) as shown in the upper panel. (D) Phosphorylation of LR2 of Pan1p in vivo. The HA-tagged LR2 immunoprecipitated from the *prk1Δ* mutant (lane a), wild-type (lane b), and wild-type cells containing the pGAL-PRK1-315 (lanes c and d) was detected by immunoprecipitation and Western blotting. Immunoprecipitates from cells containing the control vectors (pRS314 and pRS315) were used in lane e. In lane d, equal amounts of the immunoprecipitates as present in lane c were treated with CIP before being subjected to SDS-PAGE.

shown in Fig. 5 C, only the peptide with the wild-type sequence (RP15) could be strongly phosphorylated by Prk1p (Fig. 5 C, lane a). A mutation of Q to A in the LxxQxTG motif greatly reduced the phosphorylation (Fig. 5 C, lane b), indicating that the conserved Q residue in the motif was required for recognition of the phosphorylation site. Mutations of T to A and G to A in the LxxQxTG motif both completely abolished the phosphorylation of the peptide substrates (Fig. 5 C, lanes c and d), confirming the importance of these residues in the Prk1 phosphorylation site. These results show that the LxxQxTG motif is indeed the phosphorylation site of Prk1p.

After the demonstration that Prk1p could phosphorylate Pan1p in a sequence-specific manner in vitro, we then tried to investigate whether the phosphorylation of Pan1p by Prk1p could be detected in vivo. However, detection of Pan1p phosphorylation in vivo by ^{32}P-labeling proved to be difficult, as the Pan1p-specific labels in wild-type cells were at a very low level (data not shown). This effort was further hampered by prominent degradation of the Pan1 protein during immunoprecipitation (Tang and Cai, 1996; Tang et al., 1997). We subsequently found that the in vivo phosphorylation of Pan1p could be readily detected when the Prk1 kinase was overproduced. For this experiment, the LR2 region, instead of full-length Pan1p, was used because it provided better resolution of the phosphorylated and unphosphorylated bands in the gel. As shown in Fig. 5 D, the HA-tagged LR2 immunoprecipitated from wild-type cells and the *prk1Δ* mutant cells migrated as a single band (Fig. 5 D, lanes a and b). On the other hand, the same protein immunoprecipitated from cells overexpressing *PRK1* migrated as two bands (Fig. 5 D, lane c), and the upper band disappeared after treatment with CIP (Fig. 5 D, lane d). This result suggests that the LR2, which contains 10 LxxQxTG repeats, became phosphorylated in cells overproducing Prk1p.

Loss of the Kinase Activity in Prk1p Suppresses pan1-4

To obtain additional evidence for the regulation of Pan1p by the Prk1 kinase, we next sought to determine whether the genetic suppression of *pan1-4* by *prk1* involves the loss of the Prk1p kinase activity. This was important to establish, as alternative mechanisms (e.g., the loss of protein–protein binding) may also explain the suppression. To create an inactive kinase, the aspartic acid at residue 158 (D158) in Prk1p was chosen for mutagenesis because it matched the catalytic site of serine/threonine kinases (Fig. 4 A). In situ mutagenesis was used to change D158 to tyrosine. When this mutated Prk1p (Prk1p^{D158Y}) was tagged with the HA epitope, the anti-HA immunoprecipitates were found to be inactive in the kinase assay using LR1 as a substrate (Fig. 6 A, lower left). Nonetheless, the mutant kinase was expressed in vivo as well as the wild-type counterpart (Fig. 6 A, top). A plasmid containing *PRK1^{D158Y}* was used to transform the *prk1Δ pan1-4* double mutant, and the transformants were tested for temperature sensitivity at 37°C. As shown in Fig. 6 B, *PRK1^{D158Y}* was unable to restore temperature sensitivity to the double mutant, as the wild-type *PRK1* did. This result indicates that inactivation of the Prk1p kinase activity is sufficient to suppress the *pan1-4* mutation.

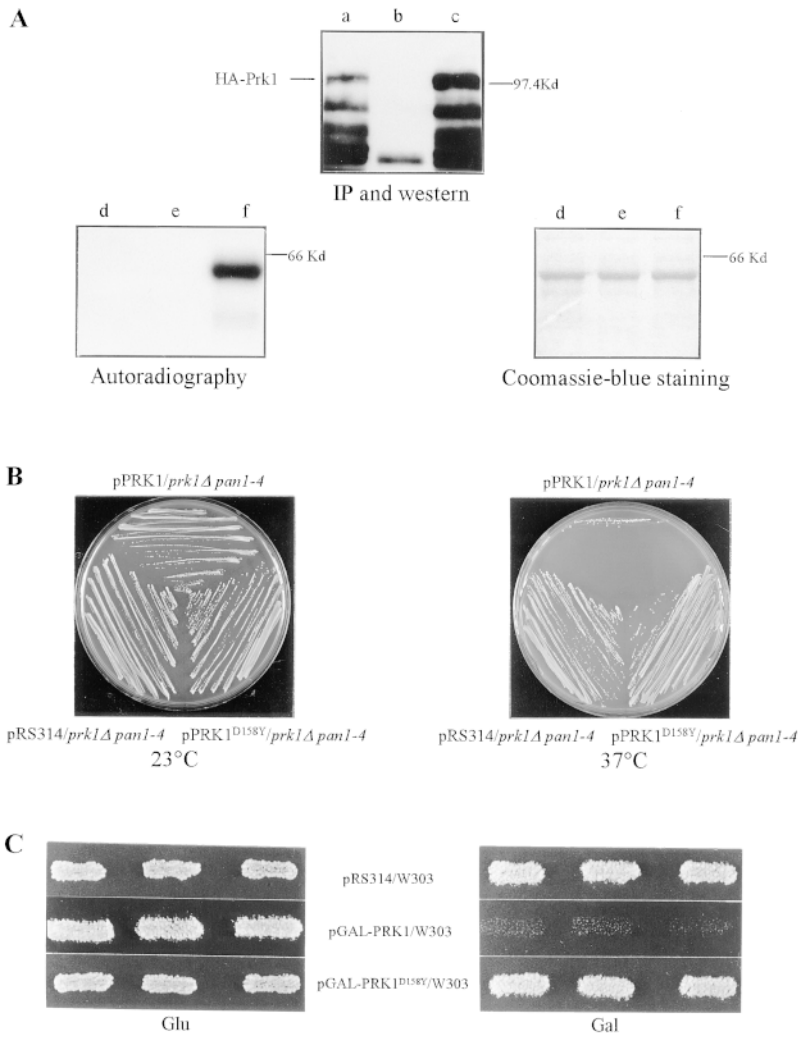

Figure 6. Characterization of Prk1p^{D158Y}. (A) Test of the kinase activity of Prk1p^{D158Y}. The HA-tagged Prk1p^{D158Y}, detectable by immunoprecipitation and Western blotting (top, lane c), was used in the kinase assay (lower left, lane d). The wild-type HA-tagged Prk1p (top, lane a) was used as a positive control in the kinase assay (lower left, lane f). Immunoprecipitates from cells containing untagged Prk1p (top, lane b) were used as negative control in the kinase assay (lower left, lane e). GST-LR1 was used as the substrate in all kinase reactions and visualized by Coomassie blue staining of the same gel as used in the kinase assay (lower right). (B) YMC425 (*prk1Δ pan1-4*) cells containing pPRK1, pPRK1^{D158Y}, and the control plasmid pRS314, respectively, were tested for growth at 23°C (left) and 37°C (right). (C) W303 cells containing pGAL-PRK1, pGAL-PRK1^{D158Y}, and the control plasmid pRS314, respectively, were tested for growth on glucose- (left) and galactose-containing plates (right).

Furthermore, the inactive Prk1p kinase was no longer lethal to cells when overproduced (Fig. 6 C). Cells containing overexpressed *PRK1^{D158Y}* also exhibited the wild-type pattern of the actin cytoskeleton (data not shown). These data suggest that the cell lethality and the actin abnormality observed in cells overproducing Prk1p both depend on the kinase activity of Prk1p.

Binding of End3p Prevents Pan1p from Being Phosphorylated by Prk1p

It was reported previously that high copy *END3* could suppress the *pan1-4* mutant phenotype (Tang et al., 1997). Pan1p and End3p have also been demonstrated to form a complex in vivo (Tang et al., 1997). In addition, *pan1-4* and *end3Δ* cells exhibited similar phenotypes including severe disorganization in the actin cytoskeleton and defects in receptor-mediated endocytosis (Tang et al., 1997). Because of the relationship between *PAN1* and *END3*, we desired to find out whether the *prk1* mutation could suppress the temperature sensitivity of *end3Δ*. The *prk1Δ end3Δ* double mutant (YMC428, Table I) was constructed and examined for temperature sensitivity. As shown in Fig. 7 A, the *end3Δ* mutation could indeed be suppressed by *prk1Δ* as the double mutant was able to grow at 37°C. Unlike the suppression of *pan1-4* by *prk1Δ*, the suppression of *end3Δ* by *prk1Δ* is the result of a bypass of *END3* function. However, *prk1Δ* could not bypass the functions of *SLA1* and *BEE1*, two other genes required for assembly of the cortical actin cytoskeleton (Holtzman et al., 1993; Li, 1997), as the temperature-sensitive phenotype in these mutants remained after the *PRK1* gene was disrupted (data not shown).

The fact that both End3p overproduction and loss of Prk1p kinase activity can suppress *pan1-4* suggests that the effects of these two factors on Pan1p are mutually antagonistic. Since End3p binds Pan1p at the LR2 region of Pan1p where several LxxQxTG repeats are present (Tang et al., 1997), it is possible that End3p protects LR2 from being phosphorylated by Prk1p. This possibility was tested in the in vitro system. Preincubation with an excess of End3p greatly diminished the LR2 phosphorylation by Prk1p, as shown in Fig. 7 B. On the other hand, the phosphorylation of LR1, which is not essential for interaction with End3p (Tang et al., 1997), was not affected under the same conditions (Fig. 7 B, left). This result suggests that Prk1p and End3p may compete with each other to regulate Pan1p function. However, we have not been able to

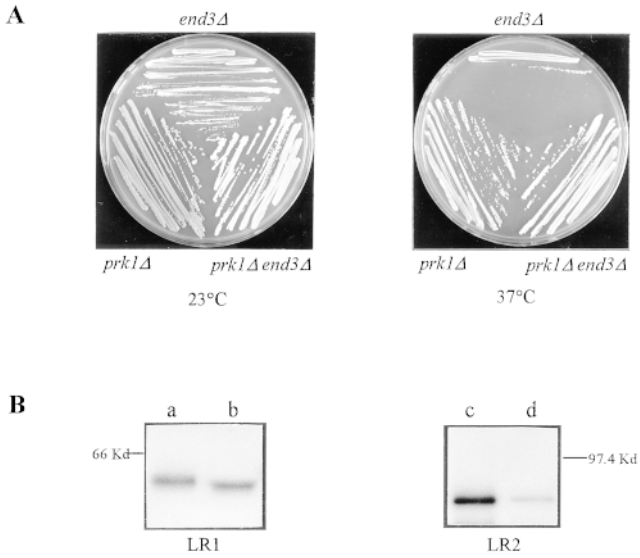

Figure 7. The antagonistic effects of End3p and Prk1p on Pan1p. (A) The suppression of the *end3Δ* temperature sensitivity by the *prk1Δ* mutation. Cells of YHT151 (*end3Δ*, Table I), YMC427 (*prk1Δ*), and YMC428 (*prk1Δ end3Δ*) were tested for growth at 23°C (left) and 37°C (right). (B) Inhibition of the Pan1p phosphorylation by End3p binding. GST-LR1 (left) and GST-LR2 (right) were preincubated either with GST (lanes a and c) or GST-END3 (lanes b and d) before being subjected to kinase assays. Equal quantities of GST-LR1 were used in lanes a and b. The same is true for GST-LR2 used in lanes c and d.

obtain conclusive data from the reciprocal experiments to test whether phosphorylation of Pan1p can inhibit the binding by End3p.

Discussion

Previous screening for mutants which exhibit a rapid death phenotype in combination with a Start-deficient mutation, *cdc28-4*, has identified Pan1p as an important protein required for proper cellular distribution of the actin cytoskeleton in yeast (Tang and Cai, 1996). To identify more factors that act with Pan1p in regulating the actin cytoskeleton, we have undertaken a genetic screen for extragenic suppressors of the temperature sensitivity of *pan1-4*. A novel serine/threonine kinase, Prk1p, has been isolated from this screen. Characterization of Prk1p suggests that this kinase is an important regulator of the actin cytoskeleton organization.

Suppression of pan1-4 by prk1

Suppression of the *pan1-4* mutation by any genetic alterations must be due to compensation for the essential function of *PAN1* lost in the mutant, since *pan1-4* is a recessive, loss-of-function, mutation (Tang and Cai, 1996; Tang et al., 1997). There are two possible mechanisms to explain the suppression of the *pan1-4* mutation by *prk1*. One is that loss of the Prk1p function may lead to hyperactivity of some proteins, which can now function in place of Pan1p to offset the deficiencies caused by the *pan1-4* mutation. Alternatively, the suppression may occur as a result of an increase in the activity of the mutant Pan1p itself, owing to a relief from the inhibitory effect imposed by the Prk1p function. The data presented in this report are in favor of the latter mechanism. Clearly, the suppression of *pan1-4* by *prk1* requires the cooperation of the mutant Pan1 protein, as the presence of *prk1* makes no difference to the absolute dependence of *pan1Δ* cells on the *PAN1* gene for viability. Furthermore, the finding that Prk1p can phosphorylate Pan1p in vitro in a sequence-specific manner also supports that Pan1p is under direct regulation of Prk1p. Therefore, we propose that the suppression of *pan1-4* by the loss of Prk1p function is more likely a result of rejuvenation of the mutant Pan1 protein than that of a bypass of the Pan1p function.

The Role of Prk1p in the Regulation of Actin Cytoskeleton Organization

The observation that the *prk1* mutant displays a randomized pattern of the cortical actin cytoskeleton at 37°C suggests that Prk1p is somehow required for the polarization of actin cytoskeleton before bud emergence. This suggestion is consistent with the mutant's phenotype of delayed bud emergence in relation to initiation of DNA replication. In addition, subcellular localization of Prk1p also supports its role in the polarization of cortical actin cytoskeleton, as the epitope-tagged Prk1p is found at the regions of cell growth such as the pre-bud site in unbudded cells and the tip of the small bud in budded cells, and appears to coincide with the polarized cortical actin patches. However, investigation of the phenotypes associated with *PRK1* overexpression indicates that the activity of Prk1p may not be limited to regulating the cortical actin polarization, as persistent overproduction of Prk1p causes gross alterations of the actin cytoskeleton organization including disruption of the normal structures and distribution of cortical patches and cytosolic cables.

How Prk1p exerts its regulation over the organization of the actin cytoskeleton remains to be elucidated. Regardless of the actual mechanism underlying the suppression of *pan1-4* by *prk1*, it is clear that the functions of Pan1p and Prk1p in the actin cytoskeleton organization are mutually antagonistic. The *pan1-4* mutant cells, similar to the Prk1p overproducing cells, typically display actin aggregates with very few normal looking actin patches present at the cell surface (Tang and Cai, 1996). Loss of Prk1p function prevents the formation of the actin aggregates, restoring not only viability at 37°C but also a virtually wild-type pattern of actin distribution to the *pan1-4* cells. As discussed above, requirement for the mutant Pan1 protein in suppression of *pan1-4* by *prk1*, and the ability of Prk1p to phosphorylate Pan1p in vitro in a sequence-specific manner advocate a direct regulation of Pan1p by Prk1p. Therefore, it follows that the function of Prk1p in the regulation of the actin cytoskeleton organization likely includes a negative regulation of the Pan1p function. It can be rationalized, for example, that the defects in *pan1-4* cells are partly due to a reduction of residual mutant Pan1p activity as a result of Prk1p phosphorylation. Introduction of the *prk1* mutation into the *pan1-4* cells alleviates such inhibition and hence restores the activity of Pan1p to the extent that its essential functions can be fulfilled.

Additional evidence to support the role of Prk1p as a negative regulator of Pan1p comes from the fact that the same allele of the *pan1* mutation, *pan1-4*, can be suppressed by either loss of Prk1p activity or overproduction of End3p (Tang et al., 1997). End3p is a functional partner of Pan1p and the protein complex containing Pan1p/End3p plays important roles in actin cytoskeleton organization and in the process of endocytosis (Tang et al., 1997). Similar to the *prk1* mutation, End3p overproduction not only suppresses the temperature sensitivity of *pan1-4*, but also restores a normal pattern of the actin cytoskeleton organization to the mutant (Tang, H., and M. Cai, unpublished data). End3p binds to the LR2 region of Pan1p where many Prk1p phosphorylation sites are present (Tang et al., 1997). Indeed, we have shown that End3p can protect the LR2 region from being phosphorylated by Prk1p in vitro. As LR2 is the essential region for Pan1p function (Sachs and Deardorff, 1992; Tang and Cai, 1996), the balance between LR2 phosphorylation by Prk1p and its binding by End3p is likely to determine the activity of Pan1p in vivo. In agreement with this, *prk1* can also suppress the temperature sensitivity of *end3Δ*, indicating that Pan1p may have become hyperphosphorylated in the absence of End3p. Despite the plausibility, however, direct evidence to support this hypothesis is still lacking.

Apart from regulating the Pan1p/End3p complex, Prk1p may also regulate the functions of other proteins involved in the actin cytoskeleton organization in yeast. To identify these potential targets of Prk1p, we have searched the yeast sequence database for proteins containing the Prk1 phosphorylation site as identified in vitro, LxxQxTG. Although the search has yielded many proteins containing one copy of this motif, few are found to contain multiple copies (data not shown). Interestingly, another protein involved in the organization of the actin cytoskeleton, Sla1p (Holtzman, et al., 1993), is found to contain five copies of the LxxQxTG repeat in its COOH-terminal region. Sla1p also shares additional sequence similarity with Pan1p in what has been named the Sla1-homology domain (Tang and Cai, 1996). Using GST-fusion proteins, the region of Sla1p that contains the LxxQxTG repeats has been found to serve as well as LR1 and LR2 as a substrate for Prk1p in vitro (data not shown), suggesting that Sla1p may be another actin cytoskeleton-related factor under the control of Prk1p.

Phosphorylation of Pan1p by Prk1p

The fact that Pan1p has the largest number of the LxxQxTG motif in its sequence among all yeast proteins suggests that it may very well be the major target of Prk1p. These short repeats are clustered within the two long repeated regions of Pan1p termed LR1 and LR2, both of which also contain an EH domain (Tang and Cai, 1996; Tang et al., 1997). We have demonstrated that the LxxQxTG motif is the site that Prk1p phosphorylates in vitro. While the importance of the L residue in the motif has not been measured, the three other residues, Q, T, and G, have been proven essential for the integrity of the phosphorylation site. We have not been able to confirm the Prk1p-dependent Pan1p phosphorylation in vivo under physiological conditions in either wild-type or the *end3* mutant cells. This difficulty may be explained by a number of reasons. It is possible, for example, that both the Prk1 and Pan1 proteins are present in low abundance in vivo. This notion is in line with the observations that the physiological levels of Prk1p and Pan1p are below detection by immunofluorescent staining, and that the overexpression of either *PAN1* or *PRK1* is detrimental to the cell (Tang and Cai, 1996; and this report). In addition, it is also conceivable that the phosphorylation of Pan1p by Prk1p in vivo may be regulated in a cell cycle–specific fashion, or coupled with protein degradation, or quickly followed by dephosphorylation, so that the phosphorylated Pan1p is unable to accumulate to a significant level in cycling cells. Whatever the reason, the finding that LR2 becomes prominently phosphorylated only in cells overproducing Prk1p suggests that Prk1p is able to recognize this region of Pan1p in vivo.

Other Considerations

We noticed that the subcellular localization of Prk1p is remarkably similar, if not identical, to that of Cdc42p, a Rho family GTPase that regulates the actin cytoskeleton polarization before bud formation (Adams et al., 1990; Johnson and Pringle, 1990; Ziman et al., 1993). We have not investigated whether the function of Prk1p requires Cdc42p and Cdc24p, a guanine-nucleotide exchange factor for Cdc42p (Zheng et al., 1994). It will be of interest to determine if, for instance, the subcellular localization of Prk1p is dependent on Cdc42p.

There are two more open reading frames in the yeast DNA sequence database that encode putative serine/threonine kinases homologous to Prk1p (Fig. 4 A). It is plausible that these Prk1-like kinases are also involved in the regulation of the actin cytoskeleton in yeast and may share certain overlapping functions with Prk1p. This could explain why *PRK1* by itself is dispensable for cell viability. This possibility has yet to be tested experimentally. There is no doubt that investigation of Prk1p, and possibly the other Prk1p-related kinases, will provide important insights into the cellular control mechanisms regulating the function of the actin cytoskeleton and its related processes.

We are grateful to Hsin-yao Tang for constructing the strains YMC422 and 423 and the plasmids GST-LR2 and pGAL-HA-LR2, and for helping with the fluorescent staining of actin in *pan1-4* cells. Jun Wang is thanked for general technical assistance. We also thank Shengcai Lin and Canhe Chen for help with optimization of GST-fusion protein production. David Botstein is thanked for providing the antiactin antibody. Catherine Pallen, Alan Munn, Hsin-yao Tang, and Mark O'Connor are thanked for their critical reading of the manuscript.

This work was supported by the Singapore National Science and Technology Board.

Received for publication 5 August 1998 and in revised form 4 December 1998.

References

Adams, A.E.M., and J.R. Pringle. 1984. Relationship of actin and tubulin distribution to bud growth in wild-type and morphogenetic-mutant *Saccharomyces cerevisiae*. *J. Cell Biol.* 98:934–945.

Adams, A.E.M., D.I. Johnson, R.M. Longnecker, B.F. Sloat, and J.R. Pringle. 1990. Two additional genes involved in budding and the establishment of cell polarity in the yeast *Saccharomyces cerevisiae*. *J. Cell Biol.* 111:131–142.

Ayscough, K.R., J. Stryker, N. Pokala, M. Sanders, P. Crews, and D.G. Drubin.

1997. High rates of actin filament turnover in budding yeast and roles for actin in establishment and maintenance of cell polarity revealed using the actin inhibitor Latrunculin-A. *J. Cell Biol.* 137:399–416.

Bénédetti, H., S. Raths, F. Crausaz, and H. Riezman. 1994. The *END3* gene encodes a protein that is required for the internalization step of endocytosis and for actin cytoskeleton organization in yeast. *Mol. Biol. Cell.* 5:1023–1037.

Benton, B.K., A.H. Tinkelenberg, D. Jean, S.D. Plump, and F.R. Cross. 1993. Genetic analysis of Cln/Cdc28 regulation of cell morphogenesis in budding yeast. *EMBO (Eur. Mol. Biol. Organ.) J.* 12:5267–5275.

Botstein, D., D. Amberg, J. Mulholland, T. Huffaker, A. Adams, D. Drubin, and T. Stearns. 1997. The yeast cytoskeleton. *In* The Molecular and Cellular Biology of the Yeast *Saccharomyces*: Cell Cycle and Cell Biology. J.R. Pringle, J.R. Broach, and E.W. Jones, editors. Cold Spring Harbor Laboratory Press, Cold Spring Harbor, NY. 1–90.

Cvrckova, F., and K. Nasmyth. 1993. Yeast G1 cyclins *CLN1* and *CLN2* and a GAP-like protein have a role in bud formation. *EMBO (Eur. Mol. Biol. Organ.) J.* 12:5277–5286.

Di Fiore, P.P., P.G. Pelicci, and A. Sorkin. 1997. EH: a novel protein-protein interaction domain potentially involved in intracellular sorting. *Trends Biochem. Sci.* 22:411–413.

Doyle, T., and D. Botstein. 1996. Movement of yeast cortical actin cytoskeleton visualized in vivo. *Proc. Natl. Acad. Sci. USA.* 93:3886–3891.

Drubin, D.G., and W.J. Nelson. 1996. Origins of cell polarity. *Cell.* 84:335–344.

Harold, F.M. 1990. To shape a cell: an inquiry into the causes of morphogenesis of microorganisms. *Microbiol. Rev.* 54:381–431.

Holtzman, D.A., S. Yang, and D.G. Drubin. 1993. Synthetic-lethal interactions identify two novel genes, *SLA1* and *SLA2*, that control membrane cytoskeleton assembly in *Saccharomyces cerevisiae*. *J. Cell Biol.* 122:635–644.

Holtzman, D.A., K.F. Wertman, and D.G. Drubin. 1994. Mapping actin surfaces required for functional interactions in vivo. *J. Cell Biol.* 126:423–432.

Johnson, D.I., and J.R. Pringle. 1990. Molecular characterization of *CDC42*, a *Saccharomyces cerevisiae* gene involved in the development of cell polarity. *J. Cell Biol.* 111:143–152.

Kilmartin, J.V., and A.E.M. Adams. 1984. Structural rearrangements of tubulin and actin during the cell cycle of the yeast *Saccharomyces*. *J. Cell Biol.* 98: 922–933.

Kron, S.J., and N.A. Gow. 1995. Budding yeast morphogenesis: signalling, cytoskeleton and cell cycle. *Curr. Opin. Cell Biol.* 7:845–855.

Lew, D.J., and S.I. Reed. 1993. Morphogenesis in the yeast cell cycle: regulation by Cdc28 and cyclins. *J. Cell Biol.* 120:1305–1320.

Lew, D.J., and S.I. Reed. 1995. Cell cycle control of morphogenesis in budding yeast. *Curr. Opin. Genet. Dev.* 5:17–23.

Lew, D.J., T. Weinert, and J.R. Pringle. 1997. Cell cycle control in *Saccharomyces cerevisiae*. *In* The Molecular and Cellular Biology of the Yeast *Saccharomyces*: Cell Cycle and Cell Biology. J.R. Pringle, J.R. Broach, and E.W. Jones, editors. Cold Spring Harbor Laboratory Press, Cold Spring Harbor, NY. 607–695.

Li, R. 1997. Beel, a yeast protein with homology to Wiscott-Aldrich syndrome protein, is critical for the assembly of cortical actin cytoskeleton. *J. Cell Biol.* 136:649–658.

Li, R., Y. Zheng, and D.G. Drubin. 1995. Regulation of cortical actin cytoskeleton assembly during polarized cell growth in budding yeast. *J. Cell Biol.* 128: 599–615.

Li, X., and M. Cai. 1997. Inactivation of the cyclin-dependent kinase Cdc28 abrogates cell cycle arrest induced by DNA damage and disassembly of mitotic spindles in *Saccharomyces cerevisiae*. *Mol. Cell. Biol.* 17:2723–2734.

Mulholland, J., D. Preuss, A. Moon, A. Wong, D. Drubin, and D. Botstein. 1994. Ultrastructure of the yeast actin cytoskeleton and its association with the plasma membrane. *J. Cell Biol.* 125:381–391.

Novick, P., and D. Botstein. 1985. Phenotypic analysis of temperature-sensitive yeast actin mutants. *Cell.* 40:405–416.

Rose, M.D., F. Winston, and P. Hieter. 1990. Methods in Yeast Genetics: A Laboratory Course Manual. Cold Spring Harbor Laboratory Press, Cold Spring Harbor, NY.

Rothstein, R. 1991. Targeting, disruption, replacement, and allele rescue: integrative DNA transformation in yeast. *Methods Enzymol.* 194:281–301.

Sachs, A.B., and J.A. Deardorff. 1992. Translation initiation requires the PAB-dependent poly(A) ribonuclease in yeast. *Cell.* 70:961–973.

Sambrook, J., E.F. Fritsch, and T. Maniatis. 1989. Molecular Cloning: A Laboratory Manual. 2nd edition. Cold Spring Harbor Laboratory Press, Cold Spring Harbor, NY.

Sikorski, R.S., and P. Hieter. 1989. A system of shuttle vectors and yeast host strains designed for efficient manipulation of DNA in *Saccharomyces cerevisiae*. *Genetics.* 122:19–27.

Tang, H., and M. Cai. 1996. The EH-domain-containing protein Pan1 is required for normal organization of the actin cytoskeleton in *Saccharomyces cerevisiae*. *Mol. Cell. Biol.* 16:4897–4914.

Tang, H., A. Munn, and M. Cai. 1997. EH domain protein Pan1p and End3p are components of a complex that plays a dual role in organization of the actin cytoskeleton and endocytosis in *Saccharomyces cerevisiae*. *Mol. Cell. Biol.* 17:4294–4304.

Thiagalingam, S., K.W. Kinzler, and B. Vogelstein. 1995. *PAK1*, a gene that can regulate p53 activity in yeast. *Proc. Natl. Acad. Sci. USA.* 92:6062–6066.

Waddle, J.A., T.S. Karpova, R.H. Waterston, and J.A. Cooper. 1996. Movement of cortical actin patches in yeast. *J. Cell Biol.* 132:861–870.

Welch, M.D., D.A. Holtzman, and D. Drubin. 1994. The yeast actin cytoskeleton. *Curr. Opin. Cell Biol.* 6:110–119.

Wendland, B., J.M. McCaffery, Q. Xiao, and S.D. Emr. 1996. A novel fluorescence-activated cell sorter-based screen for yeast endocytosis mutants identifies a yeast homologue of mammalian eps15. *J. Cell Biol.* 135:1485–1500.

Zheng, Y., R. Cerione, and A. Bender. 1994. Control of the yeast bud-site assembly GTPase Cdc42. Catalysis of guanine nucleotide exchange by Cdc24 and stimulation of GTPase activity by Bem3. *J. Biol. Chem.* 269:2369–2372.

Ziman, M., D. Preuss, J. Mulholland, J.M. O'Brien, D. Botstein, and D.I. Johnson. 1993. Subcellular localization of Cdc42p, a *Saccharomyces cerevisiae* GTP-binding protein involved in the control of cell polarity. *Mol. Biol. Cell.* 4:1307–1316.